ELSEVIER

Journal of Structural Geology 28 (2006) 2144–2155

JOURNAL OF STRUCTURAL GEOLOGY

www.elsevier.com/locate/jsg

# Topographic analysis of Devana Chasma, Venus: implications for rift system segmentation and propagation

Walter S. Kiefer [a,*], Laura C. Swafford [b,1]

[a] *Lunar and Planetary Institute, 3600 Bay Area Blvd., Houston TX 77058, USA*
[b] *Department of Geological Sciences, Michigan State University, East Lansing MI 48824, USA*

Received 16 September 2004; received in revised form 17 October 2005; accepted 6 December 2005
Available online 26 January 2006

**Abstract**

Devana Chasma is a rift system on Venus formed in association with the Beta Regio and Phoebe Regio volcanic highlands, which are interpreted as mantle plumes. We present a new analysis of a 2500-km-long segment of Devana. Based on the rift topography, the horizontal extension across the rift boundary faults is 3–9 km. This is a lower bound on the total rift extension because the altimetry does not resolve the topographic relief across the numerous faults that are visible in radar images of the rift floor. The total extension across Devana is approximately 20 km, similar in magnitude to continental rift systems on Earth. Rift flank elevations are up to 3.1 km in the regions nearest the mantle plumes and decay strongly with increasing distance from the plumes, indicating a strong thermal component to the rift flank topography, unlike the situation usually reported for terrestrial rifts. As on Earth, there is also a flexural uplift component to the flank topography. Rift depths are up to 2.5 km below the surrounding plains, with considerable along-strike variability. There is a 600 km lateral offset along Devana Chasma near the mid-point between the two mantle plumes. Devana most likely formed as two distinct rifts due to the horizontal stresses created by outflow from the upwelling plumes. The offset zone formed as a result of the interaction between the two rift tips, which requires that upwelling at the two mantle plumes overlapped in time.


*Keywords:* Venus; Devana Chasma; Rift system; Rift propagation; Rift extension; Rift flank height

## 1. Introduction

Faulted topographic troughs on Venus were first recognized in low-resolution (>10 km/pixel) radar altimetry observations made by the *Pioneer Venus Orbiter* and moderate resolution (2 km/pixel) radar imaging by the Arecibo Radio Observatory. By analogy with both the morphology and dimensions of the East African Rift system, these structures were interpreted as extensional rift systems (McGill et al., 1981; Schaber, 1982; Campbell et al., 1984; Stofan et al., 1989). In the early 1990s, NASA's *Magellan* mission significantly sharpened our view of faulting in these structures, now referred to generically as chasmata. In Devana Chasma, the impact crater Balch has been split and its two sides separated by about 10 km, confirming the extensional rift interpretation for this structure (Solomon et al., 1992). The various chasmata systems on Venus are up to 4000 km long, 150–300 km wide, and up to 5 km deep (Senske et al., 1992). Some individual normal faults within the chasmata are up to 100 km long (Foster and Nimmo, 1996).

Many of the major chasmata systems on Venus radiate away from volcanic highlands. Devana, Latona, and Zverine Chasmata are radial to Beta Regio. Ganis, Dali, Parga, Zewana, and Tkashi-mapa Chasmata are radial to Atla Regio, and Guor Linea is radial to Western Eistla Regio (Senske et al., 1992; United States Geological Survey, 1998a,b). Beta, Atla, and Western Eistla Regiones are interpreted as the surface expression of hot, upwelling mantle plumes on the basis of their large positive geoid anomalies, topographic

* Corresponding author. Tel.: +281 486 2110; fax: +281 486 2162.
*E-mail address:* kiefer@lpi.usra.edu (W.S. Kiefer).
[1] Now at: Department of Geological Sciences, Northwestern University, Evanston IL 60208, USA.

0191-8141/$ - see front matter © 2005 Elsevier Ltd. All rights reserved.
doi:10.1016/j.jsg.2005.12.002

relief, and basaltic shield volcanism (e.g. Kiefer and Hager, 1991; Smrekar et al., 1997). The mantle flow associated with such plumes produces a stress field whose orientation is consistent with the observed pattern of radially oriented rifts (Kiefer and Hager, 1991; Grimm and Phillips, 1992; Koch, 1994).

Kiefer and Peterson (2003) analyzed gravity and topography observations for Devana Chasma and Phoebe Regio and developed a model of crust and mantle density anomalies for this region. Relative to the surrounding terrain, the crust is thinned within Devana Chasma. Low density material, interpreted as hotter than normal, occurs in the mantle beneath Devana Chasma. Both observations are consistent with a rifting origin for Devana. A surprising but important aspect of their model was the observation that the mantle density anomaly is discontinuous along Devana between 7 and 10° N latitude, where Devana is laterally offset by 600 km. Within the offset region, the characteristic fault orientation is rotated by about 60° relative to the rest of the rift and there is a strong decrease in fault density. Kiefer and Peterson (2003) interpreted these observations as indicating that Devana Chasma is actually two distinct rifts. One rift propagated southward from the Beta Regio mantle plume and the second propagated northward from the Phoebe Regio mantle plume. The offset zone is the region where the stress fields from the two rift tips interacted, causing the rifts to turn toward one another.

In this work, we analyze the topography of Devana Chasma, focusing specifically on the portion of Devana Chasma between 20° N and 4° S, where Devana is located in the plains between Beta Regio and Phoebe Regio. We do not consider the northernmost part of Devana, between 20 and 33° N, where Devana crosses the summit region of Beta Regio. We address three sets of questions: (1) How much horizontal extension has Devana Chasma experienced? How does the extension vary with location along the rift? How does it compare with the extension in terrestrial rift systems? (2) How much topographic relief is there in the rift system? How does it vary with location along the rift? What is the relative importance of mantle thermal anomalies and of lithospheric flexure in supporting the rift flank topography? (3) What implications do these results have for the segmentation of the rift system and for the propagating rift hypothesis of Kiefer and Peterson (2003)? How does the rift propagation model compare with terrestrial rift systems?

## 2. Observations

### 2.1. Radar images

*Magellan* radar images of Devana Chasma (Figs. 1–3) have a resolution of 110 m/pixel in the study region. These images show the strength of the radar echo, with stronger returns being brighter. The strength of the radar return in these images is controlled primarily by two factors, the presence of oriented topographic slopes and the surface roughness (Elachi, 1987). *Magellan* was in a polar orbit around Venus, and for most of its mission its radar beam was projected to the east of the orbit track. West facing slopes, such as fault scarps, produce strong radar echos and are therefore bright in radar images. On the other hand, east facing fault scarps reflect most of the radar beam away from the spacecraft and thus are dark in radar images. If an east facing fault scarp is steep enough, it can actually create a radar shadow zone, in which the radar beam does not illuminate a portion of the floor below the scarp. The second effect that controls the appearance of these radar images is surface roughness at a scale comparable with the radar wavelength of 12.6 cm. At the incidence angles used during the *Magellan* mission, increasing the surface roughness increases the strength of the radar echo returned to the spacecraft. This effect is important for some lava flows and for impact crater ejecta blankets (e.g. crater in upper right of Fig. 2 and lava flow in lower center of Fig. 3). Mass wasting along fault scarps could also result in surface roughness and may contribute to radar brightness in the images.

Like many investigators before us (e.g. Stofan et al., 1989; Solomon et al., 1992; Foster and Nimmo, 1996; Connors and Suppe, 2001), we interpret the strong pattern of north–south oriented lineations in Figs. 1–3 as normal faults. The overall linearity of this system over several thousand kilometers favors some form of tectonic origin. The abrupt transition in radar brightness across these structures favors a scarp-like, faulted morphology; the transition in radar brightness across folds would be more gradational (Stofan et al., 1993). Some altimetry footprints for the Devana region show multiple strong returns separated by 3–5 km vertically within a single, 13 km wide footprint (Foster and Nimmo, 1996). The large elevation change within a short distance is consistent with normal faulting. Splitting of the rim of Balch crater is direct evidence for about 10 km of extension near 30° N in Devana Chasma (Solomon et al., 1992). Connors and Suppe (2001) include a detailed discussion of additional criteria for distinguishing extension and compression in Magellan radar imagery.

A regional view of our entire study region (Fig. 1) shows the dominant trend of north–south oriented faults in most of the rift system, as well as the prominent offset in the rift between 7 and 10° N latitude. Fig. 2 is a representative location in the northern part of Devana. Here, densely spaced faulting occurs over a 120-km-wide region. Within the offset region (Fig. 3), the characteristic fault strike is rotated by about 60° relative to the rest of the rift and the fault density is significantly lower than in other parts of the Devana Chasma rift system. There are no horizontally offset strain markers within the offset zone and hence no evidence for strike-slip faulting in this region.

### 2.2. Topography

The topography of Venus has been measured by radar altimetry. The horizontal resolution of these measurements varies with latitude and is best near 10° N latitude. Devana Chasma is thus ideally located for altimetry studies, with a measurement resolution of 9 km along the orbit track (effectively north–south) and 13 km in the cross track (east–west) direction (Ford and Pettengill, 1992). Rappaport et al. (1999)

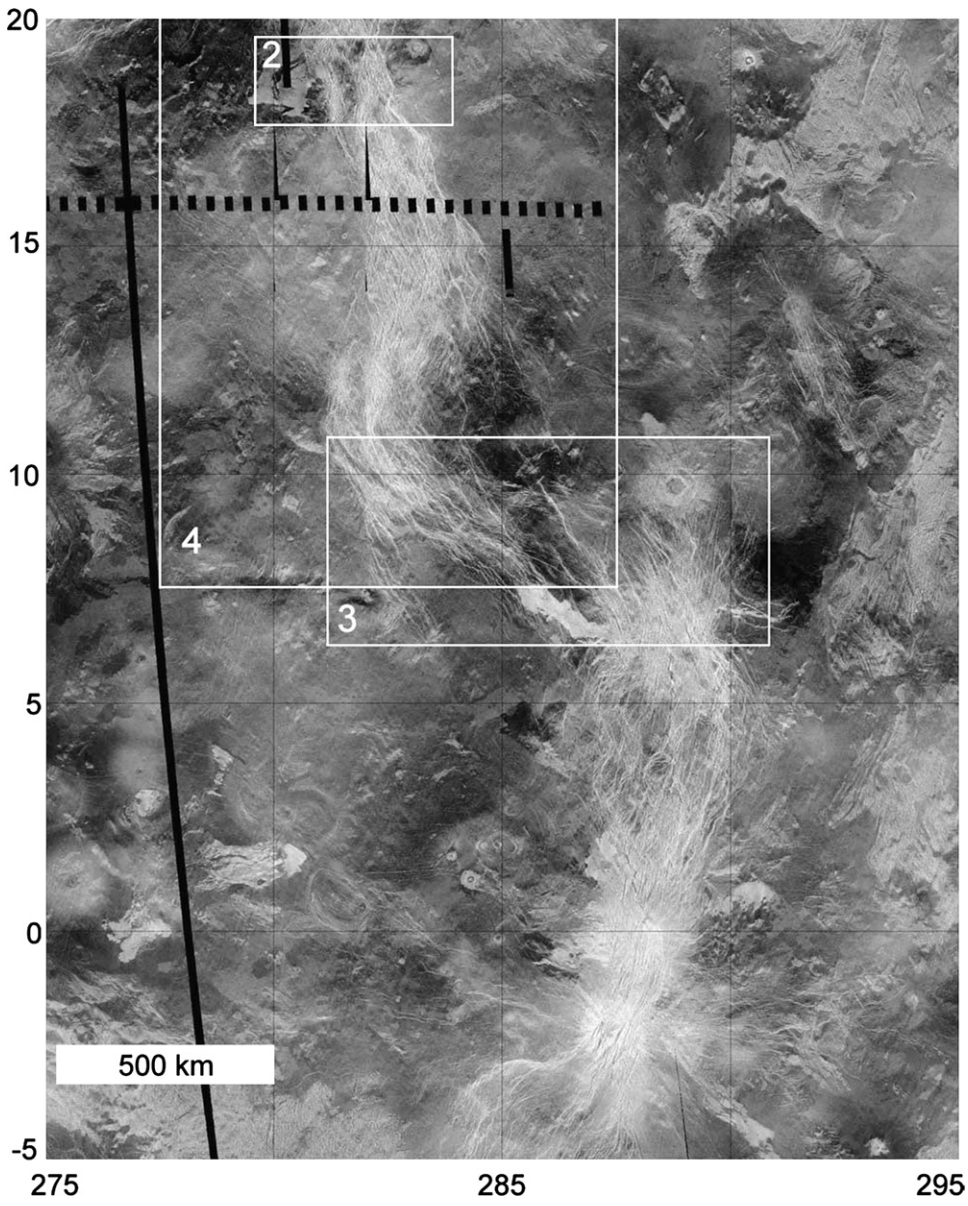


Fig. 1. Radar image of the portion of the Devana Chasma rift system studied in this paper, 5° S to 20° N latitude and 275–295° E longitude. Numbered boxes show the locations of detailed images in Figs. 2–4. The scale bar is 500 km across. Simple cylindrical projection, with north at the top.

reevaluated the altimetry data using an improved gravity model for spacecraft navigation, resulting in a considerable improvement in the quality of the topography model. *Magellan* measured the topography of Venus on three nearly complete global cycles, and Rappaport et al. (1999) estimated that the vertical error in their topography model has an RMS average of 16.1 m. The error is smallest in plains regions, where it is commonly less than 10 m. In regions of strong relief, such as Devana Chasma, the error is larger, 20–100 m, but this is still a small fraction of the topography of the rift. A shaded relief image of the topography for the northern part of our study region (Fig. 4) emphasizes both the deep topographic valley of the rift as well as the high topography on the rift flanks. The faulting visible in the Fig. 1 is largely confined to the valley floor.

In order to assess how horizontal extension and rift flank elevations varied with location along the rift, we collected a set of 97 topographic profiles from Rappaport et al.'s (1999) gridded topography model GTDR3.2. These profiles were oriented orthogonal to the rift trend and spaced at roughly 26 km intervals. Two representative examples are shown in Fig. 5, based on the profile locations shown in Figs. 2 and 3. Fig. 5a shows a well-developed rift, with flank heights of about 3.5 km and with 4 km of relief on the normal faults that bound the rift. The faulting shown in Fig. 2 is confined to the rift valley, although the altimeter's horizontal resolution is insufficient to resolve relief across individual fault scarps. In the offset region (Fig. 5b), relief within the rift is reduced to just 1.5 km and the rift flanks are virtually non-existent (note the difference in the vertical scale on the two profiles). Elevations in Fig. 5 are

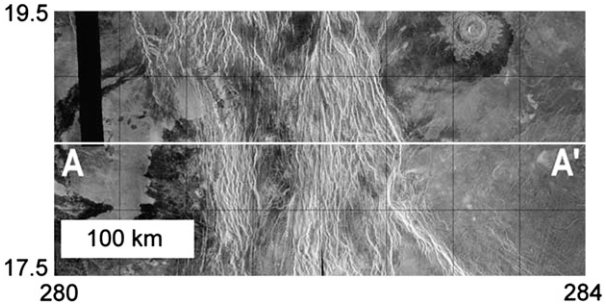


Fig. 2. Radar image of faulting in a representative portion of northern Devana Chasma. The scale bar is 100 km across. The topography for profile A–A′ is shown in Fig. 5a. Simple cylindrical projection, with north at the top.

shown in the global reference frame, referenced to the mean planetary radius of 6051.88 km (Rappaport et al., 1999)

On Earth, rift system topography is significantly modified by the deposition of sediments within rift basins. Reflection seismology results show that this sedimentary fill can be several kilometers thick (e.g. Rosendahl et al., 1992; Russell and Snelson, 1994). On Venus, the high temperature of the lower atmosphere, currently 470 °C, prevents the existence of liquid water and thus significantly limits the rate of erosion and of sediment transport. The fact that numerous faults are visible in Figs. 1–3 demonstrates that sedimentary infilling has not been a significant process at Devana Chasma. Thus, we can interpret the observed topographic profiles as effectively the topography produced by rifting.

### 2.3. Horizontal extension

We calculate horizontal extension across each topographic profile by assuming that topographic relief within the rift valley is dominantly due to normal faulting and relating vertical relief to horizontal extension via the fault dip. Thus, we calculate

$$E = \Sigma h \cot\theta, \quad (1)$$

where $E$ is the total horizontal extension, $\Sigma h$ is the sum of the vertical relief within the rift zone, and $\theta$ is the assumed fault dip. Various investigators have used similar approaches to estimate extension across graben and rift systems on Mars (Plescia, 1991; Schultz, 1995; Golombek et al., 1996). Rathbun et al. (1999) used this method to measure horizontal extension for the northern part of our study region using an earlier version of the Venus topography model. As discussed in Section 2.2, some important improvements have been made in the topography model since that time. We have therefore repeated the extension measurements for this part of Devana to ensure that we are interpreting a homogeneous set of observations.

Our extension results are shown in Fig. 6a, divided into the northern, southern, and offset portions of our study region. These results assume a nominal normal fault dip of 60°. The topographic extension is primarily between 3 and 9 km, with the largest values occurring in the northernmost portion of the study region, closest to the Beta Regio mantle plume. There are substantial along-strike fluctuations on length-scales of order 75–100 km. Similar along-strike variations in extension are observed at terrestrial rifts (Morley, 1988; Morley et al., 1992b). These fluctuations are the expected result for a system that is composed of numerous faults. Along each fault, displacement is zero at the two fault tips and reaches a maximum somewhere near the middle of the fault (Dawers et al., 1993). The total extension in the rift is the sum of the extension on the various faults, which naturally results in along-strike fluctuations in extension of the sort shown in Fig. 6a. Dawers and Anders (1995) describe an example of this for a normal fault system in California.

Several factors contribute to the uncertainty in these extension estimates, particularly uncertainties in the topography, uncertainties in the assumed fault dip angle, and the limited horizontal resolution of the topography measurements. The uncertainty in the topography is estimated to be 20–100 m in the vicinity of Devana Chasma (Rappaport et al., 1999). Assuming that the bulk of the relief and thus of the extension occurs on the two boundary fault systems (see Fig. 5a) and that

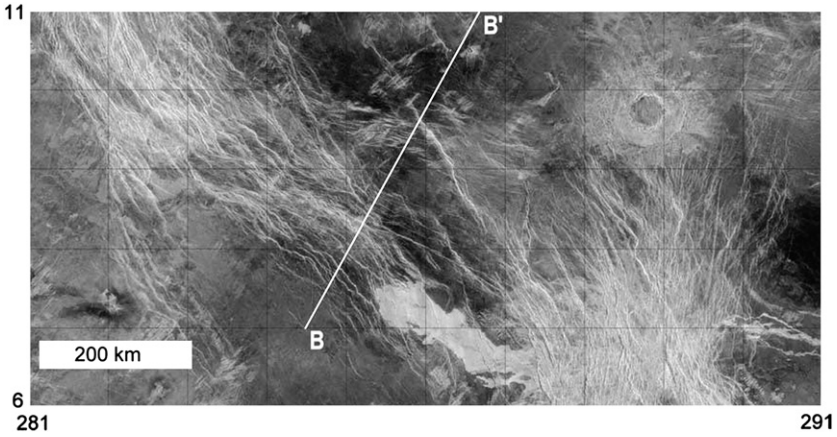


Fig. 3. Radar image of the offset in Devana Chasma. Note the strong reduction of fault density within this region relative to other parts of Devana. The scale bar is 200 km across. The topography for profile B–B′ is shown in Fig. 5b. Simple cylindrical projection, with north at the top.

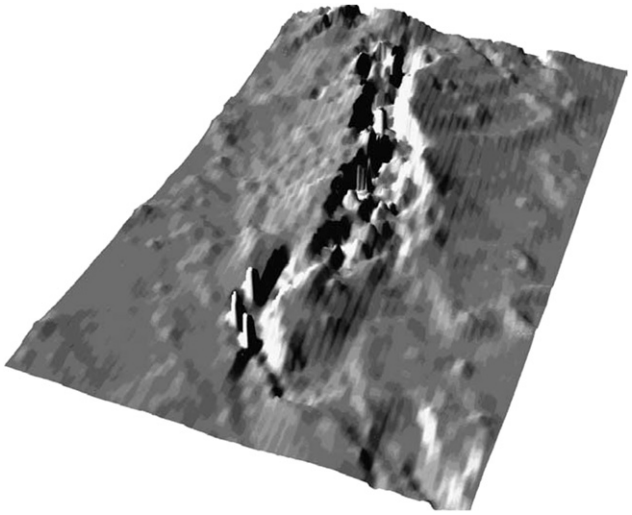

Fig. 4. Shaded relief image of the topography of the northern part of the study region, 7.5–22.5° N, 277.5–287.5° E. The image is illuminated from the west and viewed obliquely from the southeast.

the topographic errors at each point are statistically independent, the uncertainty in the extension due to topography errors is about 100–150 m, which is a small fraction of the observed extension shown in Fig. 6a. Uncertainties in the fault dip can cause larger uncertainties in the calculated extension. Schultz (1995) suggested a range of 50–70° for $\theta$ and Connors and Suppe (2001) suggested a range of 60–70°. Relative to our nominal value of 60° for $\theta$, changing the dip by 10° leads to roughly a 50% change in the calculated extension, with the extension being largest for the smallest fault dip. This introduces a significant uncertainty in the amplitude of the extension, but the pattern of extension as a function of location shown in Fig. 6a will remain robust provided that the fault dip does not vary significantly with location along the rift.

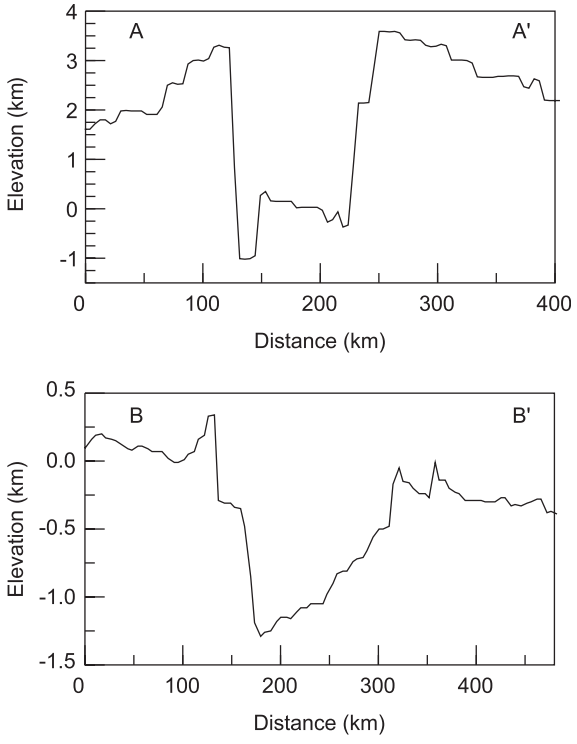


Fig. 5. (a) Topographic profile across the northern part of Devana Chasma, 18.5° N. The profile location is shown as A–A′ in Fig. 2. (b) Topographic profile across the offset zone of Devana Chasma. The profile location is shown as B–B′ in Fig. 3.

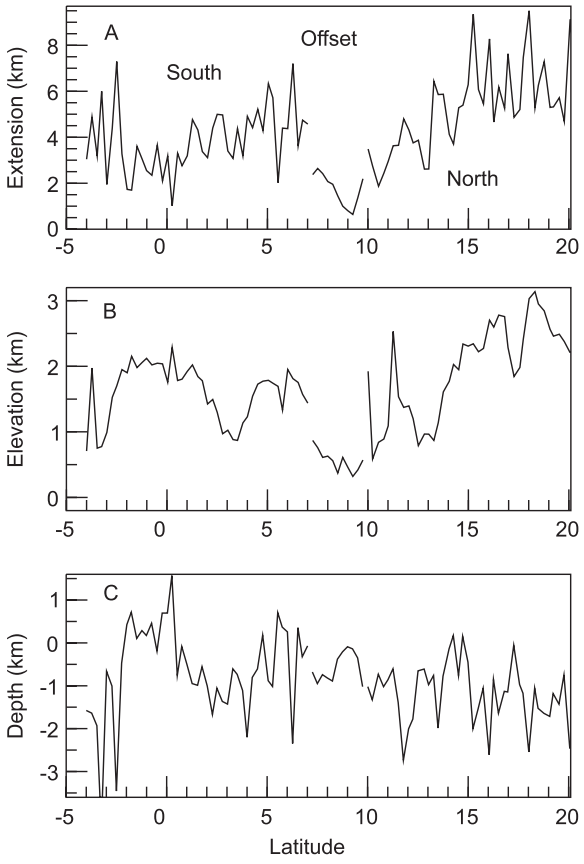


Fig. 6. Horizontal extension, rift flank heights, and rift flank depths along Devana Chasma. Results are plotted separately for the northern, southern, and offset zone segments of Devana. Because the rift strikes predominantly north–south, latitude is used as the distance coordinate for all three graphs. In the offset zone, results are plotted at the latitude that corresponds to the rift center. One degree of latitude corresponds to 105.6 km on Venus; the total distance plotted is 2535 km. (a) Horizontal extension. (b) Rift flank height. (c) Rift flank depth. Negative values indicate where the rift floor is below the surrounding plains.

The third and most important source of uncertainty in the extension measurements is the limited horizontal resolution of the altimetry, which is measured for a cell size of 9 km by 13 km (Ford and Pettengill, 1992). In contrast, the radar images have roughly two orders of magnitude higher resolution, and Fig. 2 shows the presence of densely distributed faulting on the floor of the rift. Estimates of extension based on the topography may not fully resolve extension on these rift-floor faults. As summarized in Table 1, the horizontal extension has been estimated from radar image data for four transects across Devana Chasma. This permits a test of the importance of small-scale deformation to the total extension. The southern two transects are within our study region. To permit a more comprehensive error analysis, we also calculated topographic extension estimates for profiles at the two northern transects listed in Table 1.

Table 1
Devana Chasma extension

| Latitude | Topographic extension[a] (km) | Total extension (km) | Ratio | Distance from plume center[b] (km) |
|---|---|---|---|---|
| 29.9° N | 3.5 | 10[c] | 0.35 | 200 |
| 28.6° N | 4.9 | 20.2[d] | 0.24 | 60 |
| 18.6° N | 6.7 | 11.4[d] | 0.59 | 1000 |
| 15.0° N | 6.3 | 21.8[d] | 0.29 | 1370 |

[a] Topographic extension estimated using Eq. (1).
[b] Plume center 28° N, 283° E (Kiefer and Hager, 1991).
[c] Extension of Balch Crater (Solomon et al., 1992).
[d] Connors and Suppe (2001), based on a normal fault dip of 60°.

Balch Crater is 40 km across and has experienced approximately 10 km of extension due to rifting, as indicated by the deformed and split crater rim (Solomon et al., 1992; Rathbun et al., 1999). Note that Balch is now the official International Astronomical Union name for this crater (United States Geological Survey, 1998a), although it was referred to as Somerville by some earlier researchers. Based on the topography between 282.9 and 283.4° longitude, we obtain a topographic extension of just 3.5 km. Our extension estimate is slightly less than the 4 km obtained by Rathbun et al. (1999) (value assumes $\theta$=60°) using an earlier version of the Venus topography grid.

Connors and Suppe (2001) used radar imagery to estimate extension at three transects across Devana Chasma, assuming that the fault scarps observed in the imagery originally formed at dips of 60–70° but have now collapsed to the angle of repose. Stereo images for fault scarps elsewhere on Venus indicate that the angle of repose assumption is generally appropriate, although no stereo images exist to check it specifically in Devana Chasma. For an initial fault dip of 60°, Connors and Suppe (2001) find the total horizontal extension on their transects to be 11–22 km, with uncertainties of 20–40% (see their Table 4 for transect-specific values). For these same transects, we estimate topographic extension of just 4.9–6.7 km. These differences are not due to uncertainties in the assumed fault dip, as the dip affects both methods in the same manner.

The topographic extension calculated using Eq. (1) for the four transects in Table 1 is just 24–59% of the total extension observed by Connors and Suppe (2001). In one sense, these results are somewhat discouraging because they indicate that the large-scale topographic extension measured by the altimeter is only a small to moderate fraction of the total extension in densely faulted regions. However, the topographic extension results reported here remain useful, because the topography offsets used to calculate extension are primarily due to the boundary faults on the margins of the rift. Thus, the topographic extension results in Fig. 6a essentially measure the extension on the boundary fault systems. By comparing the topographic extension and the total extension results in Table 1, we can assess the relative importance of the boundary faults and of the rift floor faults in producing rift extension. For example, our profile at 18.5° N lies very close to Transect 2 of Connors and Suppe (2001). We measure 6.7 km of topographic extension, which is almost entirely due to the boundary faults on the east and west margins of the rift (Fig. 5a). Connors and Suppe (2001) measured a total extension of 11.4 km, so 4.7 km (=11.4–6.7) of extension occurs on faults on the floor of the rift. There are roughly 50 faults that cross profile A–A′ (Fig. 2), so on average each rift floor fault accommodates about 100 m of extension. For Transects 1 and 3 of Connors and Suppe (2001) (15.0 and 28.6° N), the rift floor faults must accommodate about 15.5 km of extension in each transect, which is about three times the extension on the boundary faults.

Rathbun et al. (1999) previously measured extension for part of our study area. Their 'southern rift' consists primarily of the northern part of our measurements, between 10 and 20° N. Although their study was done with an earlier version of the global topography model, their results, like ours, show a gradual decline in extension with distance from the Beta Regio plume, and also show short length-scale oscillations in the amplitude of extension with distance along the rift. All of the extension results in their paper are corrected for the effects of small-scale faulting based on their measurement of extension at Balch crater. Table 1 shows that the correction factor (the Ratio column of the table) varies strongly with location, so their results may not actually represent the total extension in many parts of Devana Chasma. Although our study and Rathbun et al. (1999) used different versions of the topography model, this conclusion does not depend on the particular choice of topography model. Rather, there appears to be considerable along-strike variation in the amount of small-scale, rift floor extension. Thus, it is not possible to use a simple, multiplicative constant to relate large-scale, topographic extension to total extension. Table 1 also suggests that there is no simple relationship between the ratio (topographic extension/total extension) and distance from the plume center.

Finally, we note that within the offset zone between 7 and 10° N, the measured extension is much less than elsewhere along the rift, generally less than 2 km and sometimes less than 1 km. Moreover, the extension in the offset zone is discontinuous with the extension measured further south along the rift. The density of faulting is low in the offset zone, particularly in the central part of the offset (Fig. 3). This indicates that the small-scale faulting does not make a large contribution to the total extension in the offset zone and that the topographic extension is likely to be close to the total extension in the offset region.

### 2.4. Rift flank heights and rift depth

Rift flank elevations as a function of location along the rift are shown in Fig. 6b. The results presented here are the average of the east and west rift flanks at each location along the rift. The plains surrounding the rift are used as the reference elevation for rift flank height and rift depth in Fig. 6, with the reference elevation at each point along the rift being averaged at distances of 400–600 km from the rift flank. Because of the broad distribution of high topography close to the volcanic rises, it is difficult to determine an accurate reference elevation near the northern and southern limits of our study

region. As a result, we suspect that we have underestimated the rift flank heights in the regions between 18–20° N and 3–4° S. Similarly, the rift depths in these regions probably are shallower than shown in Fig. 6c.

The rift flanks are highest, 3.1 km, near the northern end of the rift, closest to the Beta Regio mantle plume, which is centered near 28° N, 283° E (Kiefer and Hager, 1991). The strong decrease in topography to the south between 18 and 13° N latitude is consistent with the topography having a large component of thermal support, which would naturally decrease in strength with increasing distance from the mantle plume, although the local fluctuations between 10 and 12° N do not fit into this framework. The flank topography along the southern segment of the rift has a smaller peak elevation than in the north (2.3 km versus 3.1 km). The southern rift flank topography also shows less variability with distance along the rift than is seen in the north. Gravity modeling indicates that the Beta Regio plume remains active (Kiefer and Hager, 1991; Smrekar et al., 1997; Rathbun et al., 1999), whereas the Phoebe Regio mantle plume appears to be waning in strength (Kiefer and Peterson, 2003). The results of Fig. 6b are consistent with this interpretation.

Within the offset zone of the rift, 7–10° N, the rift flanks are quite low, typically less than 600 m and always less than 900 m in height. The pattern of flank elevations shown in Fig. 6b strongly suggests that the offset zone is a distinct segment of the rift, separate from both the northern and southern segments. Kiefer and Peterson (2003) concluded that there was little or no hot upper mantle in the offset region, although the strength of that conclusion was somewhat limited by the resolution of the gravity data that they modeled. The limited rift flank topography within the offset zone is additional evidence for the absence of hot lithosphere beneath the offset zone and demonstrates that Kiefer and Peterson's (2003) conclusion was not an artifact of the gravity resolution.

The maximum rift depth varies significantly with location along the rift (Fig. 6c), with negative values indicating that the rift floor is below the elevation of the surrounding plains, which were used as the reference surface. The northern part of the rift is deepest on average, occurring primarily between −1 and −2.5 km. The southern portion of the rift is typically somewhat shallower than the northern segment of the rift. In parts of the southern segment, the rift floor is actually higher in elevation than the adjacent plains (positive depth in Fig. 6c). The offset zone is not distinguishable from the northern and southern segments of the rift on the basis of its depth, a situation that is unlike the case for rift flank elevation. The deepest section of Devana Chasma, −3.3 km with respect to the global reference frame of mean planetary radius, is among the lowest elevations anywhere on Venus.

## 3. Discussion

### 3.1. Rift extension on Venus and Earth

Extension in terrestrial rift systems is sometimes reported as a percent strain, with the observed extension normalized by the width of the extended region. Devana Chasma is typically 150–300 km wide, which is significantly broader than terrestrial continental rifts (Foster and Nimmo, 1996). This would artificially reduce the percent strain for Devana in comparison with terrestrial rifts. Thus, we prefer to compare Devana with terrestrial rifts by directly comparing horizontal extension measured for the various rifts.

Extension in terrestrial continental rifts has been measured by a variety of methods, including reflection seismology, flexural modeling of gravity and topography profiles, field mapping, and measurements of basin topographic subsidence. Table 2 summarizes results for a variety of locations, including the Rio Grande Rift of New Mexico and Colorado, the Main Ethiopian Rift, both the Eastern and Western branches of the East African Rift system, and the Gulf of Suez. In these regions, extension due to rifting varies between 5 and 40 km. The 11–22 km of extension observed in Devana Chasma on Venus (Connors and Suppe, 2001) is thus comparable with the extension that occurs in present-day terrestrial continental rifts. The expected rift extension is a function of the imposed stress and of the lithosphere's strength, with high stresses and weak lithospheres favoring increased extension. Numerical modeling of mantle plumes indicates that the plume-related stresses on Venus are likely to be a factor of about three larger than on Earth (Kiefer and Hager, 1991). On the other hand, the crust of Venus is basaltic and dry; both factors increase the strength of the Venus lithosphere (Mackwell et al., 1998) relative to the wet, more siliceous rocks that typify the Earth's crust. These two effects roughly offset each other, and it is therefore not particularly surprising that the extension in Devana Chasma is similar in magnitude to that at terrestrial rifts.

### 3.2. Sources of rift flank topography

There are three principal factors that contribute to producing rift flank topography: volcanic construction, flexural uplift,

Table 2
Terrestrial Rift extension

| Location | Extension (km) | References |
|---|---|---|
| San Luis Basin, Rio Grande Rift | 5–8 | Kluth and Schaftenaar (1994) |
| North Albuquerque Basin, Rio Grande Rift | 6.5 | Russell and Snelson (1994) |
| South Albuquerque Basin, Rio Grande Rift | 12–13 | Russell and Snelson (1994) |
| Southern Main Ethiopian Rift | 12–25 | Ebinger et al. (1993) |
| Turkana Basin, Kenya Rift | 25–40 | Morley et al. (1992a) and Hendrie et al. (1994) |
| Central Kenya Rift | Minimum 8-10 | Hendrie et al. (1994) |
| North Albert Basin, Western Branch of East African Rift ('Western Rift') | 6 | Upcott et al. (1996) |
| South Albert Basin, Western Rift | 7 | Upcott et al. (1996) |
| Edward Basin, Western Rift | 9 | Upcott et al. (1996) |
| Tanganyika Basin, Western Rift | 4.5 | Morley (1988) |
| Rukwa Basin, Western Rift | 10 | Morley et al. (1992b) |
| Central Gulf of Suez | 25–27 | Steckler (1985) |
| Southern Gulf of Suez | 30 | Steckler et al. (1988) |

and thermal or dynamic uplift. In Devana Chasma, volcanic construction is not a significant factor along most of the rift. The strongest contribution from volcanic construction is in the vicinity of 2° S, 287° E, where comparisons of radar imagery and altimetry profiles indicates that a shield volcano contributes about 500 m to the rift flank topography.

Flexural uplift of rift flanks is a consequence of the development of the rift valley, which serves as a negative load on the lithosphere. Because of the finite elastic strength of the lithosphere, the isostatic rebound associated with rift valley formation is spread into the surrounding terrain, resulting in topographic highs that flank the rift valley (Weissel and Karner, 1989; Kusznir and Ziegler, 1992). Flexural uplift of rift flanks is important at most terrestrial rifts, including the East African Rift (Ebinger et al., 1991), the Rio Grande Rift (Brown and Phillips, 1999), and the Baikal Rift (van der Beek, 1997). In the Devana Chasma region, the elastic lithosphere is estimated to be 10–30 km thick on the basis of gravity admittance modeling (Simons et al., 1997; Barnett et al., 2000). Thus, one would anticipate that some flexural uplift of the rift flanks occurs at Devana Chasma.

Thermal or dynamic topography at rift zones is the result of buoyant uplift due to the presence of hot, low-density material in the lithosphere and upper mantle. This type of rift flank topography is not commonly discussed for terrestrial rifts. However, seismic and gravity observations of the Sierra Nevada mountains, which form the western flank of the Basin and Range extensional province, indicate that hot, low-density mantle supports more than half of the total topography (Jones et al., 1994; Liu and Shen, 1998). On Venus, the upper mantle viscosity structure is such that the mantle couples more strongly to the lithosphere, producing more dynamic topography than on Earth (Kiefer and Hager, 1991). Thus, it is reasonable to suspect that thermal topography may be important along rift systems on Venus. Indeed, in Section 2.4 we showed that the rift flank height varies systematically with distance from the Beta Regio mantle plume, which indicates that there is a significant component of thermal topography along the rift.

We therefore consider the relative importance of thermal uplift and flexural uplift in supporting the rift flank topography. One way to distinguish between these two sources of topography is to consider a scatter plot of rift flank heights versus rift depths, as shown in Fig. 7. Consider the case of purely flexural support for the rift flanks. In that case, a region with a small displacement on the rift boundary fault (a small total load on the lithosphere) results in a small depth for the rift and a small adjacent rift flank. Increasing the boundary fault displacement increases the total load on the lithosphere, which simultaneously makes the rift deeper and the rift flanks higher, both expressed relative to the plains adjacent to the rift. Thus, in a flexural system, we expect there to be a negative correlation between rift flank height and rift depth. On the other hand, thermal support for the rift topography raises both the rift flanks and the rift floor with respect to the adjacent plains, causing a positive correlation between flank height and floor depth.

The correlation between the maximum rift flank height and the rift depth is shown as a scatter plot in Fig. 7. Both rift flank height and rift depth are expressed relative to the elevation of the plains adjacent to the rift. Results are shown separately for the northern (Fig. 7a) and southern (Fig. 7b) portions of Devana Chasma. The best-fitting line for the northern observations has a slight negative slope, while the best-fitting line for the southern observations has a slight positive slope. However, the data are quite scattered and one can have little confidence in the sign of the correlation for either region. One way to produce such highly scattered data would be if thermal uplift and flexural uplift made similar overall contributions to the topography. This suggests that Devana Chasma, unlike many terrestrial rifts, has a significant thermal uplift component to its topography in addition to the flexural component. This result supports the conclusion that we reached in Section 2.4 on the basis of the variation of topography with distance from Beta Regio. It is also consistent with the gravity results of Kiefer and Peterson (2003), who demonstrated the presence of low density, presumably hotter than normal, material in the mantle beneath Devana Chasma.

### 3.3. Rift system segmentation and propagation

The topography and tectonic observations in this paper, when combined with the gravity results of Kiefer and Peterson (2003), strongly support the view that Devana Chasma has three distinct segments. The northern segment, north of

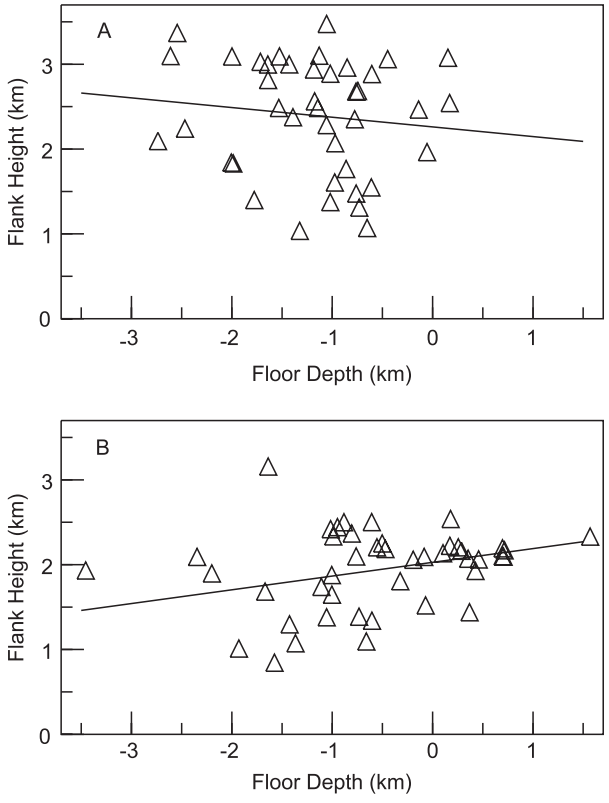


Fig. 7. Scatter plot of the maximum rift flank height versus the rift depth. Individual data points are shown as triangles. The solid lines are least-squares best fitting trend lines. (a) Results for the northern part of the rift (10–20° N). (b) Results for the southern part of the rift (4° S–7° N).

10° N latitude, is connected with Beta Regio. The amplitude of rift flank topography as a function of distance along the rift indicates the presence of a strong component of thermally uplifted topography, and the gravity observations indicate that this buoyant support is in the lower lithosphere or upper mantle. The southern segment, south of 7° N latitude, is connected with Phoebe Regio. Again, the gravity observations require the presence of buoyant support in the lower lithosphere or upper mantle. Finally, the offset segment, 7–10° N, is tectonically distinct in a variety of ways from both the northern and southern segments. First, in this region the trend of the rift is laterally offset by 600 km. Second, the fault strikes are reoriented by about 60° relative to the regions to the north and south. Third, the density of faulting is significantly reduced, and this is associated with a substantial decrease in rift extension. Finally, both the gravity observations and the absence of rift flank topography in this region indicate that there is little or no hot material in the lower lithosphere and upper mantle beneath the offset zone.

These relationships are best understood when interpreted in terms of the Beta Regio and Phoebe Regio mantle plumes. Gravity observations and mantle flow modeling indicate that both Beta and Phoebe are locations of hot, upwelling mantle flow (e.g. Kiefer and Hager, 1991; Smrekar et al., 1997; Rathbun et al., 1999; Kiefer and Peterson, 2003; Vezolainen et al., 2003). When the upwelling material reaches the base of the thermal lithosphere, it flows laterally outward away from the plume. Because of the increasing area with increasing distance from the plume center, streamlines of the flow diverge from one another as they flow away from the plume, creating extensional stresses in the overlying lithosphere. In a locally cylindrical coordinate frame centered on the plume, the azimuthal stress $\sigma_{\varphi\varphi}$ is more extensional than the radial stress $\sigma_{rr}$ (Kiefer and Hager, 1991; Koch, 1994). This results in rifts oriented radial to the plume center, as observed at both the northern and southern segments of Devana Chasma and elsewhere on Venus. Presumably, each rift forms initially near the upwelling when the plume first approaches the lithosphere. As the plume head spreads laterally outward away from the plume axis, the rift also propagates away from the plume axis. Formation of the rift in a propagating manner is energetically preferred, as it requires less total driving force than if the rift were to be formed simultaneously along its entire length (Parmentier and Schubert, 1989). Lateral outflow of plume material from a mantle plume has also been invoked to account for the pattern of volcanism and tectonism in east and central Africa (Ebinger and Sleep, 1998).

In this model, the offset zone between 7 and 10° N is a region of interaction between the two rift tips, where the superposition of the two rift tip stress fields alters the preferred direction of faulting. Visually, the reorientation of the fault direction in this zone (Fig. 3) resembles the theoretical rift tip interactions calculated by Pollard and Aydin (1984). The closest terrestrial analog that we are aware of is the interaction of crack tips along segments of fast-spreading mid-ocean ridges (Macdonald et al., 1991). These characteristically occur at scales of a few kilometers to tens of kilometers, one to two orders of magnitude smaller than the Devana Chasma case. Pollard and Aydin (1984) documented terrestrial examples of crack tip interaction over eight orders of magnitude in length scale, so the additional size increase on Venus is not an enormous problem. The crucial issue in determining whether the two rift tips are able to interact is the ratio of the rift tip offset (600 km for Devana Chasma) to the horizontal length scale of the rifts. In the purely elastic model of Pollard and Aydin (1984), the appropriate length scale is the length of individual rift faults (about 100 km for Devana Chasma; Foster and Nimmo, 1996). In the elastic model, the separation ratio is about 6, which is far too large for the rift tips to interact via their stress fields. However, as we noted above, the stresses that are ultimately responsible for producing the rift are due to the viscous outflow of the plume head just below the base of the lithosphere. In this case, a plausible choice of length scale for the stress field is the plume head radius, of order 1000–1500 km for both Beta Regio and Phoebe Regio. With this choice of scaling, the separation ratio is of order 0.4–0.6, which would permit significant interaction between the stress fields of the two rift tips. No quantitative modeling exists of the rift tip stresses in the combined viscous flow plus elastic lithosphere model. The visual pattern of faulting in Fig. 3 strongly suggests some sort of rift tip stress field interaction, and we therefore favor using the plume head radius as the appropriate length-scale for scaling the stress field. If our rift tip interaction hypothesis is correct, it implies that upwelling at the Beta and Phoebe mantle plumes must have overlapped in time. Future three-dimensional modeling of the interaction between the stress fields of two spreading plume heads would be computationally complex but would improve our knowledge of the dynamics of this system. For example, such models might be able to test our hypothesis that the plume head radius is an appropriate length scale for controlling the stress interaction.

Other explanations for the deflection of Devana Chasma are possible, although we consider them less likely. One possibility is that cold, strong lithosphere deflects the trend of the rift into areas of weaker, more easily faulted lithosphere. This occurs, for example, in the East African Rift, which bifurcates around the strong, Archean Tanzania craton to produce the Kenya Rift and the Western Rift (Nyblade and Brazier, 2002). Modeling of the gravity and topography for Devana Chasma suggests the possibility that the mantle surrounding the offset zone is 40–50 K colder than average (Kiefer and Peterson, 2003), which might provide some support for the lithospheric strength heterogeneity model. However, the pattern of mantle cold anomalies in their map parallels the edges of the much stronger high temperature anomalies along the Devana Chasma rift. This suggests that the cold anomalies are in fact the result of ringing due to the spherical harmonic degree 40 cut-off used in that gravity modeling. Gravity modeling of the Tuulikki Mons shield volcano west of the rift offset zone indicates that the elastic lithosphere there is just 8 km thick (Kiefer and Potter, 2000). To the northeast of the rift offset, highly faulted tessera terrain is also inconsistent with

abnormally strong, fault-resistant lithosphere. Collectively, these observations indicate that the pattern of faulting in Devana is not primarily controlled by large heterogeneities in lithospheric strength.

Guor Linea is a rift system associated with the Western Eistla Regio volcanic rise. Guor has a prominent bend in the rift's trend near 18° N, 3° E. Grimm and Phillips (1992) explained the bend in Guor as due to the interaction of outflow from plumes at Western Eistla and Central Eistla, which results in some unspecified way in an asymmetry in the north and south outflows and thus causes a rotation of the trend of Guor. They mapped a variety of fault sets (labeled sets A–K, their fig. 3) in Western Eistla. The primary component of Guor, which extends beyond their mapped region, is radial to a point midway between the shield volcanoes Gula Mons and Sif Mons in Western Eistla. Based on its volcanism, tectonism, geoid anomaly, and topography, Western Eistla Regio is likely the site of an upwelling mantle plume (Grimm and Phillips, 1992; Senske et al., 1992; Smrekar et al., 1997). Thus, we interpret most of Guor as caused by stresses from the outflow of the plume head, in a manner analogous to the northern and southern segments of Devana Chasma. Part of the bend in Guor is due to fault set B, which is radial to Gula Mons, a 2.5-km-high shield volcano with a basal diameter of 300 km. Similar radially oriented faults occur around other parts of Gula. We interpret fault set B as due to the superposition of volcanic loading stresses with the plume head stresses. This volcanic loading origin cannot be applied to the bend in Devana Chasma, as there is no suitable lithospheric load in the vicinity of Devana's bend. The final part of Guor's bend is fault sets A1 and A3. These are a group of parallel faults in a fault field that is 800 km across, so their association with Guor in one portion of the fault field may be coincidental. This interpretation of Guor Linea indicates that the bend in Guor should not be used as a counterexample to our rift tip interaction model for Devana Chasma.

A possibly more significant counterexample is Ganis Chasma, a rift system connected to the Atla Regio volcanic rise on Venus (Senske et al., 1992). Like Devana, Ganis initially strikes radial to the volcanic highland, and we interpret it as formed by plume-related stresses. Near 16° N, 197° E, the trend of the rift rotates roughly 50° westward. Faulting associated with Ganis Chasma terminates in the plains northwest of Atla Regio and there is no evidence that a second plume is involved, so the rift tip interaction model developed for Devana cannot be applied to Ganis. This rotation might be controlled by stresses related to other aspects of the global mantle convection system on Venus or by local lithospheric strength heterogeneities. Unfortunately, Ganis has only been briefly described in the early survey of Senske et al. (1992) and we therefore cannot assess the possible causes of the rift reorientation in Ganis at this time. Detailed analysis of the tectonic structures, topography, and gravity anomalies along Ganis and comparison with Devana would improve our overall knowledge of rifting on Venus and may serve as an additional test of the rift tip interaction model.

## 4. Conclusions

We have analyzed topography profiles and radar images for a 2500-km-long segment of the Devana Chasma rift system on Venus. Based on our observations, we have reached the following major conclusions:

(1) The horizontal extension across the rift boundary faults is between 3 and 9 km, depending on the location along the rift. This is a lower bound on the total extension across the rift, because the altimetry does not resolve the topographic relief across most of the faults on the floor of the rift. In three regions, independent measurements of fault deformation on radar images indicate a total extension of 11–22 km (Connors and Suppe, 2001). In these three locations, the total extension on the rift floor faults is between one and three times as large as the extension on the boundary faults. The total extension across Devana is comparable with that observed at continental rifts on Earth.
(2) The rift flanks have a maximum elevation of 3.1 km near Beta Regio and 2.3 km near Phoebe Regio. The amplitude of the rift flank topography decays with increasing distance from the Beta Regio mantle plume, indicating a strong thermal component to the rift topography, which differs from most terrestrial rifts. Gravity observations along the rift are consistent with this interpretation. A flexural uplift component is also present along Devana Chasma. Volcanic construction plays only a limited role in producing rift flanks along Devana.
(3) Based on its topography, tectonics, and gravity anomaly, Devana Chasma can be divided into three distinct segments. The northern segment, north of 10° N, formed due to stresses from the Beta Regio mantle plume. The southern segment, south of 7° N, formed due to stresses from the Phoebe Regio mantle plume. In the intermediate region between 7 and 10° N, the rift has a 600 km lateral offset, a 60° reorientation in fault direction, a strong reduction in fault density, a substantial decrease in horizontal extension, and minimal rift flanks. This offset zone most likely formed due to the interaction of the stress fields from the two rift tips. For this interaction to have occurred, upwelling at the Beta Regio and Phoebe Regio mantle plumes must have overlapped in time. Future numerical modeling of the interactions between two plume heads and their stress fields, as well as comparative analysis of the Ganis Chasma rift system, may provide additional tests of the rift tip interaction model.

## Acknowledgements

We thank Peter Ford for access to the updated topography model, Brian Fessler for assistance with processing the topography model and for developing Fig. 4, and Patrick McGovern for helpful discussions. Review comments by David Ferrill, Bob Grimm, and an anonymous reviewer improved the clarity of the manuscript. This work was performed at the Lunar and Planetary

Institute, which is run by the Universities Space Research Association under NASA Cooperative Agreement NCC5-679. LCS was supported by the LPI Undergraduate Internship Program. Lunar and Planetary Institute Contribution 1215.

## References


Barnett, D.N., Nimmo, F., McKenzie, D., 2000. Elastic thickness estimates for Venus using line of sight accelerations from Magellan cycle 5. Icarus 146, 404–419.

Brown, C.D., Phillips, R.J., 1999. Flexural rift flank uplift at the Rio Grande rift, New Mexico. Tectonics 18, 1275–1291.

Campbell, D.B., Head, J.W., Harmon, J.K., Hine, A.A., 1984. Venus: volcanism and rift formation in Beta Regio. Science 226, 167–170.

Connors, C., Suppe, J., 2001. Constraints on magnitudes of extension on Venus from slope measurements. Journal of Geophysical Research 106, 3237–3260.

Dawers, N.H., Anders, M.H., 1995. Displacement–length scaling and fault linkage. Journal of Structural Geology 17, 607–614.

Dawers, N.H., Anders, M.H., Scholz, C.H., 1993. Growth of normal faults: displacement–length scaling. Geology 21, 1107–1110.

Ebinger, C.J., Sleep, N.H., 1998. Cenozoic magmatism throughout east Africa resulting from impact of a single plume. Nature 395, 788–791.

Ebinger, C.J., Karner, G.D., Weissel, J.K., 1991. Mechanical strength of extended continental lithosphere: constraints from the Western Rift system, East Africa. Tectonics 10, 1239–1256.

Ebinger, C.J., Yemane, T., Woldegabriel, G., Aronson, J.L., Walter, R.C., 1993. Late Eocene–Recent volcanism and faulting in the southern Main Ethiopian Rift. Journal of the Geological Society London 150, 99–108.

Elachi, C., 1987. Introduction to the Physics and Techniques of Remote Sensing. John Wiley and Sons, New York.

Ford, P.G., Pettengill, G.H., 1992. Venus topography and kilometer-scale slopes. Journal of Geophysical Research 97, 13,103–13,114.

Foster, A., Nimmo, F., 1996. Comparisons between the rift systems of East Africa, Earth, and Beta Regio, Venus. Earth and Planetary Science Letters 143, 183–195.

Golombek, M.P., Tanaka, K.L., Franklin, B.J., 1996. Extension across Tempe Terra, Mars, from measurements of fault scarp widths and deformed craters. Journal of Geophysical Research 101, 26,119–26,130.

Grimm, R.E., Phillips, R.J., 1992. Anatomy of a Venusian hot spot: geology, gravity, and mantle dynamics of Eistla Regio. Journal of Geophysical Research 97, 16,035–16,054.

Hendrie, D.B., Kusznir, N.J., Morley, C.K., Ebinger, C.J., 1994. Cenozoic extension in northern Kenya: a quantitative model of rift basin development in the Turkana region. Tectonophysics 236, 409–438.

Jones, C.H., Kanamori, H., Roecker, S.W., 1994. Missing roots and mantle "drips": regional $P_n$ and teleseismic arrival times in the southern Sierra Nevada and vicinity, California. Journal of Geophysical Research 99, 4567–4601.

Kiefer, W.S., Hager, B.H., 1991. A mantle plume model for the Equatorial Highlands of Venus. Journal of Geophysical Research 96, 20,947–20,966.

Kiefer, W.S., Peterson, K., 2003. Mantle and crustal structure in Phoebe Regio and Devana Chasma, Venus. Geophysical Research Letters 30 (1), 1005, doi:10.1029/2002GL015762.

Kiefer, W.S., Potter, E.-K., 2000. Gravity anomalies at Venus shield volcanos: implications for lithospheric thickness. Lunar Planetary Science Conference 31, Abstract 1924.

Kluth, C.F., Schaftenaar, C.H., 1994. Depth and geometry of the northern Rio Grande Rift in the San Luis Basin, south-central Colorado. In: Keller, G.R., Cather, S.M. (Eds.), Basins of the Rio Grande Rift: Structure, Stratigraphy, and Tectonic Setting. Geological Society of America Special Paper 291, pp. 27–37.

Koch, D.M., 1994. A spreading drop model for plumes on Venus. Journal of Geophysical Research 99, 2035–2052.

Kusznir, N.J., Ziegler, P.A., 1992. The mechanics of continental extension and sedimentary basin formation: a simple-shear/pure-shear flexural cantilever model. Tectonophysics 215, 117–131.

Liu, M., Shen, Y., 1998. Sierra Nevada uplift: a ductile link to mantle upwelling under the Basin and Range province. Geology 26, 299–302.

Macdonald, K.C., Scheirer, D.S., Carbotte, S.M., 1991. Mid-ocean ridges: discontinuities, segments, and giant cracks. Science 253, 986–994.

Mackwell, S.J., Zimmerman, M.E., Kohlstedt, D.L., 1998. High-temperature deformation of dry diabase with application to tectonics on Venus. Journal of Geophysical Research 103, 975–984.

McGill, G.E., Steenstrup, S.J., Barton, C., Ford, P.G., 1981. Continental rifting and the origin of Beta Regio, Venus. Geophysical Research Letters 8, 737–740.

Morley, C.K., 1988. Variable extension in Lake Tanganyika. Tectonics 7, 785–801.

Morley, C.K., Wescott, W.A., Stone, D.M., Harper, R.M., Wigger, S.T., Karanja, F.M., 1992. Tectonic evolution of the northern Kenya Rift. Journal of the Geological Society London 149, 333–348.

Morley, C.K., Cunningham, S.M., Harper, R.M., Wescott, W.A., 1992. Geology and geophysics of the Rukwa Rift, East Africa. Tectonics 11, 69–81.

Nyblade, A.A., Brazier, R.A., 2002. Precambrian lithospheric controls on the development of the East African Rift system. Geology 30, 755–758.

Parmentier, E.M., Schubert, G., 1989. Rift propagation. Geophysical Research Letters 16, 183–186.

Plescia, J.B., 1991. Graben and extension in northern Tharsis, Mars. Journal of Geophysical Research 96, 18,883–18,895.

Pollard, D.D., Aydin, A., 1984. Propagation and linkage of oceanic ridge segments. Journal of Geophysical Research 89, 10,017–10,028.

Rappaport, N.J., Konopliv, A.S., Kucinskas, A.B., Ford, P.G., 1999. An improved 360 degree and order model of Venus topography. Icarus 139, 19–31.

Rathbun, J.A., Janes, D.M., Squyres, S.W., 1999. Formation of Beta Regio, Venus: results from measuring strain. Journal of Geophysical Research 104, 1917–1927.

Rosendahl, B.R., Kilembe, E., Kaczmarick, K., 1992. Comparison of the Tanganyika, Malawi, Rukwa and Turkana Rift zones from analyses of seismic reflection data. Tectonophysics 213, 235–256.

Russell, L.R., Snelson, S., 1994. Structure and tectonics of the Albuquerque Basin segment of the Rio Grande Rift: insights from reflection seismic data. In: Keller, G.R., Cather, S.M. (Eds.), Basins of the Rio Grande Rift: Structure, Stratigraphy, and Tectonic Setting. Geological Society of America Special Paper 291, pp. 83–112.

Schaber, G.G., 1982. Venus: limited extension and volcanism along zones of lithospheric weakness. Geophysical Research Letters 9, 499–502.

Schultz, R.A., 1995. Gradients in extension and strain at Valles Marineris, Mars. Planetary Space Science 43, 1561–1566.

Senske, D.A., Schaber, G.G., Stofan, E.R., 1992. Regional topographic rises on Venus: geology of Western Eistla Regio and comparison to Beta Regio and Atla Regio. Journal of Geophysical Research 97, 13,395–13,420.

Simons, M., Solomon, S.C., Hager, B.H., 1997. Localization of gravity and topography: constraints on the tectonics and mantle dynamics of Venus. Geophysical Journal International 131, 24–44.

Smrekar, S.E., Kiefer, W.S., Stofan, E.R., 1997. Large volcanic rises on Venus. In: Bougher, S.W., Hunten, D.M., Phillips, R.J. (Eds.), Venus II: Geology, Geophysics, Atmosphere, and Solar Wind Environment. University of Arizona Press, Tucson, pp. 845–878.

Solomon, S.C., Smrekar, S.E., Bindschadler, D.L., Grimm, R.E., Kaula, W.M., McGill, G.E., Phillips, R.J., Saunders, R.S., Schubert, G., Squyres, S.W., Stofan, E.R., 1992. Venus tectonics: an overview of Magellan observations. Journal of Geophysical Research 97, 13,199–13,255.

Steckler, M.S., 1985. Uplift and extension at the Gulf of Suez: indications of induced mantle convection. Nature 317, 135–139.

Steckler, M.S., Berthelot, F., Lyberis, N., Le Pichon, X., 1988. Subsidence in the Gulf of Suez: implications for rifting and plate kinematics. Tectonophysics 153, 249–270.

Stofan, E.R., Head, J.W., Campbell, D.B., Zisk, S.H., Bogomolov, A.F., Rzhiga, O.N., Basilevsky, A.T., Armand, N., 1989. Geology of a rift zone on Venus: Beta Regio and Devana Chasma. Geological Society of America Bulletin 101, 143–156.

Stofan, E.R., Senske, D.A., Michaels, G., 1993. Tectonic features in Magellan data. In: Ford, J.P., Plaut, J.J., Weitz, C.M., Farr, T.G., Senske, D.A.,

Stofan, E.R., Michaels, G., Parker, T.J. (Eds.), Guide to Magellan Image Interpretation. NASA Jet Propulsion Laboratory Publication 93-24, pp. 93–108.

United States Geological Survey, 1998a. The Guinevere Planitia Region of Venus. U.S. Geological Survey Map I-2457, scale 1:10,000,000.

United States Geological Survey, 1998b. The Helen Planitia Region of Venus. U.S. Geological Survey Map I-2477, scale 1:10,000,000.

Upcott, N.M., Mukasa, R.K., Ebinger, C.J., Karner, G.D., 1996. Along-axis segmentation and isostasy in the Western Rift, East Africa. Journal of Geophysical Research 101, 3247–3268.

van der Beek, P., 1997. Flank uplift and topography at the central Baikal Rift (SE Siberia): a test of kinematic models for continental extension. Tectonics 16, 122–136.

Vezolainen, A.V., Solomatov, V.S., Head, J.W., Basilevsky, A.T., Moresi, L.-N., 2003. Timing of formation of Beta Regio and its geodynamical implications. Journal of Geophysical Research 108 (E1), doi:10.1029/2002JE001889.

Weissel, J.K., Karner, G.D., 1989. Flexural uplift of rift flanks due to mechanical unloading of the lithosphere during extension. Journal of Geophysical Research 94, 13,919–13,950.